Electrocatalysis (2017) 8:279–287
DOI 10.1007/s12678-017-0367-9

ORIGINAL RESEARCH

An Artificial Photosynthesis System Based on Ti/TiO_2 Coated with Cu(II) Aspirinate Complex for CO_2 Reduction to Methanol

Simone Stülp[1] · Juliano C. Cardoso[2] · Juliana Ferreira de Brito[2] · Jader Barbosa S. Flor[2] · Regina Célia Galvão Frem[2] · Fabiana Avoilo Sayão[2] · Maria Valnice Boldrin Zanoni[2]

Published online: 9 March 2017

Abstract A novel copper(II) aspirinate complex easily deposited onto nanotubes of Ti/TiO_2 was successfully employed in the conversion of CO_2 to methanol through the use of UV-Vis irradiation coupled to a bias potential of −0.35 V vs saturated calomel electrode. An average concentration of 0.8 mmol L^{-1} of methanol was obtained in 0.1 mol L^{-1} of sodium sulfate saturated with CO_2 using a self-organized Ti/TiO_2 nanotubular array electrode coated with a $[Cu_2(asp)_4]$ complex. The influence exerted by CO_2 and the complex over the behavior of photocurrent vs potential curves is discussed. Furthermore, a complete investigation of all parameters that tend to influence the global process of methanol production by the photoelectrocatalytic method such as applied potential, electrolyte, and time is also thoroughly presented.

Keywords CO_2 reduction · Copper aspirinate complex · Methanol · Photoelectrocatalysis · Artificial photosynthesis

Introduction

The reduction of carbon dioxide emitted into the atmosphere has become a global pressing environmental challenge given its harmfully significant contribution to the greenhouse effect, which leads to global warming [1–3]. Most commonly, the process involving carbon dioxide reduction in the atmosphere entails the following: (i) the capture of carbon dioxide, followed by (ii) its transportation and storage or (iii) its conversion to useful products in an affordable manner. Among the available possibilities regarding its conversion into useful products, the transformation of CO_2 into synthetic hydrocarbon fuels has gained considerable attention [4–6].

In this context, the photoconversion of CO_2 is a theme of high interest in artificial photosynthesis, where molecular species can be used to produce energy from sunlight, generating a useful fuel for storage and mobile use [7]. Some examples that merit mentioning include photovoltaic cells based on inorganic or organic semiconductors for the production of electricity, dye-sensitized solar cells, systems for fuel production based on such devices, and devices for fuel production associated with the use of an organic or inorganic photocatalyst besides other related systems [7]. A wide range of materials are used aiming at facilitating the reduction of CO_2, including centers for fast proton transfer, semiconductor with higher light absorption, and efficient charge separation, among others [8].

The use of p-type semiconductors such as ZnO, CdSe, ZrO_2, Ga_2O_3, and doped TiO_2 as photocatalysts in the process of CO_2 reduction has brought meaningful contributions to this area [9–14]. The photocatalytic process involves the photoirradiation of the catalyst surface that promotes the generation of e^-/h^+ charges where the excited electron in the conduction band could migrate to the surface and, by so doing, actively contributes towards reducing CO_2 to hydrocarbon derivatives (CO, CH_4, CH_3OH, and HCOOH). Recently, reports have been published regarding the use of photoelectrocatalysis combining photocatalysis with bias potential which has improved the efficiency of CO_2 photoreduction [5, 15, 16]. Specifically, some electrode materials have been reported to have contributed towards improving the selectivity of CO_2/alcohol conversion and amplifying the

✉ Juliano C. Cardoso
jcarvalho82@gmail.com

[1] Centro Universitário Univates, Rua Avelino Tallini, 171, Bairro Universitário, Lajeado, RS 95900-000, Brazil

[2] Instituto de Química de Araraquara, Universidade Estadual Paulista "Júlio de Mesquita Filho" (UNESP), R. Prof. Francisco Degni, 55, P.O. Box 355, Araraquara, SP 14800-900, Brazil

quantum yield, resulting in the diminishing of the charge recombination.

An alternative pathway towards the conversion of CO_2 involves the use of the copper complex as a molecular photocatalyst [13, 17–20]. A large part of the results that have been published indicates partial reduction and points out mainly to the formation of CO.

TiO_2 is one of the most successful materials used in photoelectrocatalysis [21] thanks to its essential features including the fact that it is economic, environmentally friendly, presents long lifetime of electron/hole pairs, and has compatible energy position of BV and BC, good chemical and thermal stability, and superior catalytic stability. Yet, notwithstanding these relevant good characteristics, the applicability of TiO_2 when it comes to reduction processes is found to be limited [22]. Taking into account that copper complexes represent a relatively good choice as electrocatalysts capable of reducing CO_2 to higher oxidation states, the coupling of TiO_2 with copper complexes of low cost, besides being environmentally friendly and easy to prepare, could aid in enhancing the electron transfer processes in CO_2 photoreduction while contributing towards improving the selectivity of the formed products. The copper(II) aspirinate complex was chosen as a catalyst model as a result of its antioxidant and anti-inflammatory properties, superoxide scavenging activities, and easy synthesis [23, 24]. It is known that the complex can be easily deposited onto nanotube TiO_2 electrodes and used as mediator of electron transfer during nitrite reduction [25].

The present work reports the photoelectrocatalytic behavior of the TiO_2 nanotube electrode modified with deposits of the copper(II) aspirinate complex (chemical structure in Fig. 1) and its influence on photocatalytic conversion of CO_2 in aqueous solution. The photoconversion was carried out in a photoelectrocatalytic reactor combining UV/Vis irradiation, and a bias potential is capable of engendering the formation of alcohols monitored by gas chromatographic techniques.

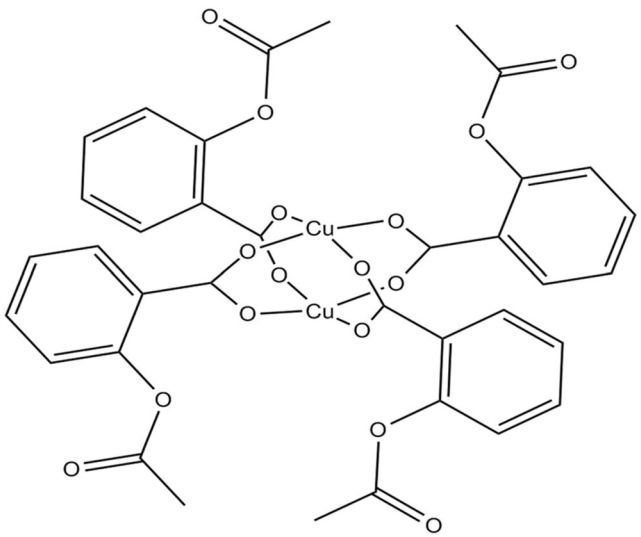

Fig. 1 Copper aspirinate structure

Experimental

Synthesis of the Copper(II) Aspirinate Complex

The copper(II) aspirinate complex, $[Cu_2(asp)_4]$, was prepared, in line with the procedures reported in the literature [1], as follows: 4.5 g of acetylsalicylic acid was suspended in 50 mL of distilled water and stirred at 60 °C using a magnetic bar. Afterwards, about 1.5 g of solid copper(II) carbonate was slowly added, and at the end, the solution was left stationary for 15 min prior to filtration. The greenish blue crystals were washed with ice-cold distilled water and dried at room temperature. The structure of $[Cu_2(asp)_4]$ was confirmed using X-ray and elemental analyses while being subjected to comparison with reports in the literature [24, 26]. Ultra-pure reagents were purchased from Merck, and purified water derived from a Millipore Milli-Q system (resistivity 18.2 mΩ cm, pH 6.9) was used in the preparation of all solutions.

Decoration of TiO_2 Nanotube Arrays with Cu(II) Aspirinate

The nanostructured TiO_2 electrodes were prepared by anodic oxidation processes of titanium sheets and through glycerol/water mixture in the presence of NH_4F as a supporting electrolyte followed by annealing at 450 °C for 60 min, as described previously [27–30]. The nanotubular surfaces were coated with copper aspirinate using two methodologies, namely, spin coating and electrochemical deposition.

Spin Coating

A solution of 20 mmol L^{-1} of Cu(II) aspirinate in dimethyl sulfoxide was subjected to ultrasound for 20 min. Approximately 400 μL of this solution was placed on the cleaned TiO_2 nanotube surface (6 cm^2 of area) and left for 60 s under 400 rpm rotation followed by a further 30 s under 4000 rpm. The electrodes were subsequently dried at 80 °C for 10 min, and this procedure was considered as one deposition step. Briefly, the final coating was obtained after three steps following the same procedure.

Electrochemical Processes

The immobilization of $[Cu_2(asp)_4]$ on the TiO_2 nanotube electrode was also carried out via electrochemical deposition. The cleaned electrode was introduced into an electrochemical cell containing a solution of 5×10^{-4} mol L^{-1} of complex in 0.1 mol L^{-1} Na_2SO_4 at pH 4, where oxygen was removed

by bubbling nitrogen gas for 10 min. The electrode was subjected to cycling in the potential range of +0.5 V to −0.5 V under a scan rate of 100 mV s^{-1} (100 cycles).

Characterization of the Electrodes

The morphological characterization was undertaken through field emission gun-scanning electron microscopy (FEG-SEM) with a JEOL 7500F microscope. The optical properties were evaluated by diffuse reflectance spectroscopy (DRS), using a UV/Vis/NIR spectrometer (PerkinElmer Lambda 1050) with an integrating sphere 150-mm UV/Vis/NIR (InGaAs) Module. The equipment was calibrated with a Spectralon standard (Labsphere USRS-99-020, 99% reflectance), and the reflectance was measured in the range of 250–800 nm. The electronic properties of all electrodes were evaluated by photocurrent curves via the linear sweep voltammetry (−0.2 to 1.0 V) technique at ν = 10 mV s^{-1} in 0.1 mol L^{-1} Na_2SO_4 solution (Sigma-Aldrich), under dark and UV/Vis irradiation (lamp of 125 W of Hg high pressure). In addition, the electronic properties were evaluated using chronoamperometric technique with UV/Vis light on and off.

Photoelectrochemical Reactor

A photoelectrochemical reactor with two compartments interconnected by a single porous glass plate at a temperature of 25 °C controlled by a thermostatic bath (Quimis, Brazil) was used to promote the reduction of CO_2 [31]. In the cathodic compartment, the TiO_2 nanotubes (NTs) bare and modified with copper aspirinate used as working electrode along with a reference electrode Ag/AgCl in KCl 3 mol L^{-1} were placed at a distance of 5 cm from a quartz tube containing a mercury lamp of 125 W high pressure. In the other compartment, a DSA electrode was positioned as counter electrode. For the photoelectrocatalytic (PEC) process, the working electrode was subjected to a constant potential of −0.35 V for 3 h. For the photocatalysis processes (PCs), only the electrode was used in the photoreactor with a UV lamp. The photoelectroreduction of CO_2 was conducted using 150 mL of supporting electrolyte containing dissolved carbon dioxide through bubbling of the gas (OXI-MEDIN). The CO_2 reduction was carried out, and aliquots were removed after a specified time and analysis by gas chromatography.

Chromatographic Analysis

Methanol and ethanol were analyzed by gas chromatography using a gas chromatograph GC-FID model CP-3800 Varian, where the reduced CO_2 solution was subjected to a solid-phase microextraction technique (SPME). In the procedure adopted for the SPME technique, a fiber covered with a thin selective layer that extracts the alcohol directly from aqueous samples before injection into the gas chromatograph was used [26]. To this end, 0.5 mL of the photoelectrolyzed solution was transferred to a properly closed container (1.5 mL) and subjected to heating in a bath using IKA brand model HB 0.5 0.6 CN for 7 min. The fiber was in turn exposed to the vapor for 5 min and injected into the gas chromatograph. A chromatographic column consisting of 30 m Stabilwax Restek Columns with 0.25 mm internal diameter and 25 μm film thickness was used along with nitrogen, as the carrier gas, at a flow rate of 1.0 mL min^{-1}. The temperature employed for the injector and detector was 250 °C. The heating ramp was 35 °C for 4 min, at 45 °C at 1 °C min^{-1}, at 120 °C at 20 °C min^{-1}, and finally at 120 °C for 4.5 min. Calibration curves for methanol and ethanol determination were constructed with a linear relationship from 0.5 to 40 ppm, $r = 0.97517$ and $r = 0.99307$, respectively. The detection limits obtained were 0.45 ppm and 0.15 for methanol and ethanol, respectively.

Results and Discussion

Characteristics of the Electrode

Figure 2 illustrates the FEG-SEM images obtained for TiO_2 NTs prior to (A) and following deposition of $[Cu_2(asp)_4]$ using one (B), two (C), and three (D) spin coatings. The formation of organized and perpendicular tubes positioned on the Ti surface can be observed with tubes around 1.5 μm of length, 90 nm of diameter, and 10 nm of wall thickness. The formation of a smooth deposition of copper aspirinate around the tubes is seen after the first coating, which increases with new depositions covering a large area of the surface after three successive coatings where the tube filling is observed in the cross section image shown in the inset of Fig. 2e. Figure 2f depicts the electrochemical deposition image.

The XRD pattern of TiO_2 NT coating with three different deposits of $[Cu_2(asp)_4]$ by spin coating is shown in Fig. 3. The diffraction peaks at about 2θ—25.5°, 37.3°, 38.1°, 48.2°, 54.2°, and 55.2°—can be indexed to the (101), (103), (004), (200), (105), and (211) crystal phases of anatase TiO_2. Anatase form is found to be preponderant in the composition of TiO_2 nanotubular electrodes which are electrochemically prepared. The diffraction peak at 35.1° can be indexed to the part of $[Cu_2(asp)_4]$ (002). The XRD pattern obtained for TiO_2 NTs coated with electrochemical deposition of $[Cu_2(asp)_4]$ presented a similar behavior.

Figure 4 shows the UV-visible absorption spectra of all electrodes synthesized: TiO_2 NT and TiO_2 NT coated by one, two, and three depositions of $[Cu_2(asp)_4]$ using spin coating and also via electrochemical deposition. The spectra exhibited no significant variation in the absorption behavior of the synthesized materials. Diffuse reflectance curves also

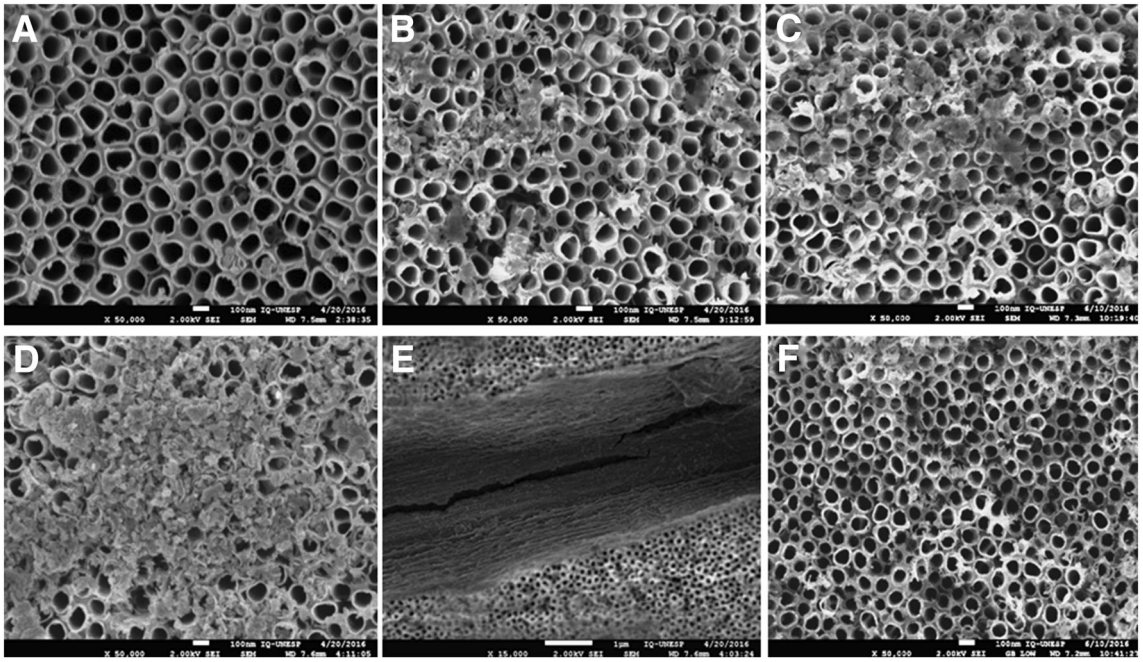

Fig. 2 FEG-SEM of TiO_2 nanotube arrays. Bare TiO_2 NTs (**a**); 1 cycle (**b**); 2 cycles (**c**); 3 cycles (**d**) of spin coating deposition of copper aspirinate (II); cross-section view of 3 cycles of deposition (**e**) and electrochemical deposition (**f**)

showed a similar behavior, and the band gap energy values were calculated based on these curves using the Kubelka-Munk function $(F(R)E)^{1/2}$ and photon energy (h). The values obtained were 3.1 eV for all modified materials and 3.2 eV for bare TiO_2 NTs. This behavior essentially indicates that the deposition of the complex does not play any interfering role as far as the optical properties of the material are concerned. The absorption spectra for the $[Cu_2(asp)_4]$ complex powder can also be seen in the inset of Fig. 4. A broad absorption band was observed between 200 and 800 nm with the highest absorption seen at 500 nm [32, 33]. The direct transition of 1.90 eV was estimated based on the Kubelka-Munk function. This behavior illustrates that the $[Cu_2(asp)_4]$ complex powder has visible light absorption and low band gap, where three possible mechanisms are associated with the formation of photogenerated holes involving $3d^9$ (i) $d_{x2\text{-}y2} \rightarrow d_{xy}$, (ii) $d_{x2\text{-}y2} \rightarrow d_{z2}$, and (iii) $d_{x2\text{-}y2} \rightarrow d_{zx,\ yz}$ [32].

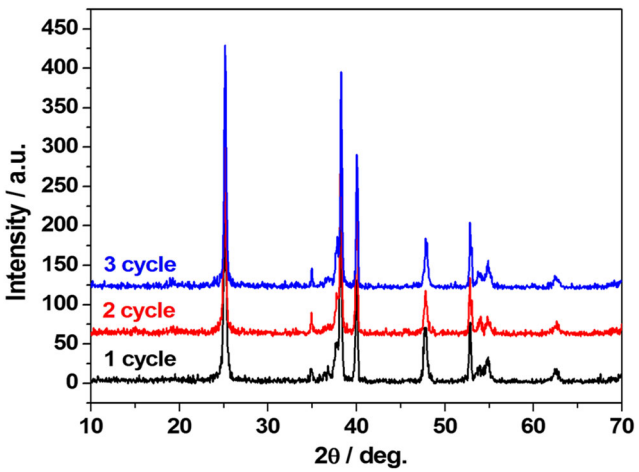

Fig. 3 XRD patterns of TiO_2 NTs coating with $[Cu_2(asp)_4]$ after 3 cycles using the spin coating technique

Effect of the Complex on the Photoactivity of the Ti/TiO_2 Nanotube Electrode

Figure 5 illustrates the curves of linear scan voltammograms showing the influence of the complex, UV irradiation, and CO_2

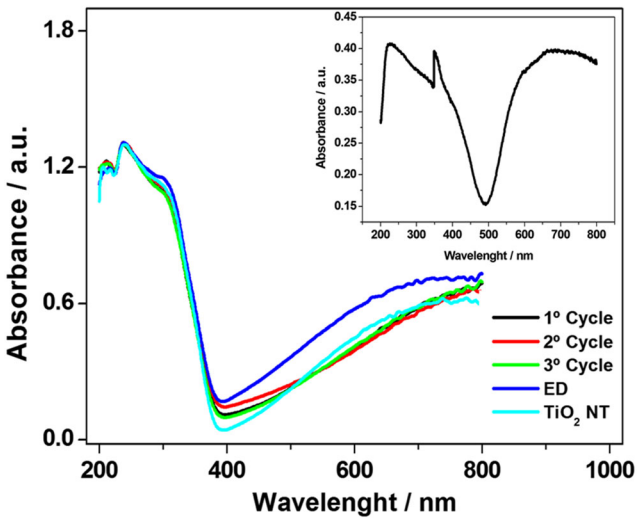

Fig. 4 UV-visible absorption spectra of all electrodes synthesized by spin coating and electrochemical deposition including TiO_2 NT arrays. 1°cycle (*black*); 2°cycles (red); 3°cycles (*green*); electrodeposited (*blue*); and bare TiO_2 NTs (*cyan*). *Inset graphic*: absorption spectra of copper aspirinate

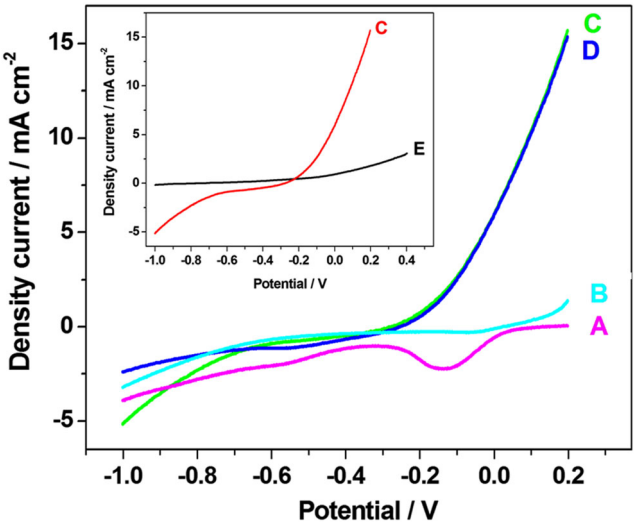

Fig. 5 Linear scan voltammograms of TiO_2 NT coating with $[Cu_2(asp)_4]$ after 1 cycle. *A* Without CO_2 and light off. *B* With CO_2 and light off. *C* With CO_2 and light on. *D* Without CO_2 and light on. *E* TiO_2 NTs bare light on

dissolved in the electrolyte in the photoactivity of the Ti/TiO_2 electrode in 0.1 mol L^{-1} sodium sulfate. In the dark, the comparison of curves A and B illustrates the effect of the complex, where a well-defined peak is observed around −0.12 V assigned to the reduction of Cu(II) from the copper aspirinate complex to Cu(I) deposited on TiO_2, which does not show any peak in the same region. In addition, a slight shoulder is seen close to −0.6 V, where probably the metallic center of the complex is reduced to copper (0). This hypothesis was confirmed by voltammetric studies carried out on vitreous carbon electrode, where the peaks are well-defined around close potentials (results not shown here). Under UV irradiation, both electrodes were found to raise the currents higher to a more positive potential superior to −0.35 V (Fig. 5c, d) for TiO_2-$[Cu_2(asp)_4]$ and −0.048 V (Fig. 5e) for Ti/TiO_2, which essentially indicates that under UV irradiation there is a greater separation of e^-/h^+ generated using the modified electrode, leading to a higher photocurrent. Moreover, the process is facilitated on the modified electrode as a result of a shift of a flat band of 0.3 V and the current is increased to at least 3.4×10^{-3} mA cm^{-2}.

Ti/TiO_2-$[Cu_2(asp)_4]$ in the presence of CO_2 (Fig. 5c) in the dark presented a decline in the copper reduction peak of the complex at −0.35 V, while under UV irradiation, the curve exhibited higher currents at a more positive potential superior to −0.3 V. This fact can be attributed to CO_2 ability to capture the electron promoted to the conduction band on the Ti/TiO_2 modified with the copper aspirinate complex which acts as electron trap. Thus, the current increase observed in curves C and D of Fig. 5 can be associated with the presence of the modifier metal inserted both in and between the TiO_2 nanotubes.

Aiming at a deeper investigation of the abovementioned effects, further experiments of photocurrent responses in the light on-off process were performed. Figure 6 illustrates the performance of the Ti/TiO_2-$[Cu_2(asp)_4]$ electrode in sulfate solution with and without saturation with CO_2 at 0 V, where good photoresponses and reproducibility were verified for varying on-off cycles under the light on and light off conditions. The Ti/TiO_2-$[Cu_2(asp)_4]$ sample exhibited higher photocurrents compared to those observed for the bare electrode under UV-Vis irradiation and applied potential of 0 V, in the medium with CO_2. The complex hydrolyzes in solution at a pH higher than 6, but it is very stable when deposited at the Ti/TiO_2 electrode surface at pH 7.0, which was chosen for further experiments. The leaching losses of the complex were verified only after 75 h of experiments, and after such reduction, new depositions were performed.

Figure 6a compares the photocurrent recorded for both Ti/TiO_2-$[Cu_2(asp)_4]$ coated by spin coating and photoelectroreduction in a solution containing CO_2. Higher photocurrent transients have relatively higher spikes on the modified electrode as compared to the Ti/TiO_2 NT electrodes, suggesting that the copper complex can act as an electron mediator of CO_2 reduction as verified previously [9, 13, 18–20].

Figure 6b shows the photocurrent of Ti/TiO_2-$[Cu_2(asp)_4]$ spin coating electrodes in the presence and absence of CO_2. In the CO_2-saturated electrolyte, photocurrent transients for Ti/TiO_2-$[Cu_2(asp)_4]$ are found to be close to two times higher than in the N_2-saturated solution. These results confirm that in the presence of CO_2, the recombination of charges is better minimized given the fact that CO_2 is being indirectly reduced by the electrons mediated by the complex on the semiconductor surface.

Ti/TiO_2-$[Cu_2(asp)_4]$ electrodes prepared by electrodeposition and via spin coating (one, two, and three depositions) were also compared in Fig. 6c, d in the presence and absence of CO_2. Higher photocurrents were obtained when the Ti/TiO_2 electrode is coated with the copper complex through spin coating. For comparison purposes, the photocurrent is found to increase successively with the number of coatings. Admittedly though, smaller photocurrents are observed when the deposit of the complex is carried out via electrochemical reduction. This behavior is indicative that perhaps the redox state of the metallic center undergoes a change during the electrochemical cyclization, and probably the best performance observed is propelled by the copper(II) aspirinate.

Performance of Ti/TiO_2-$[Cu_2(asp)_4]$ Electrodes in CO_2 Reduction

In order to test the efficiency of Ti/TiO_2-$[Cu_2(asp)_4]$ electrodes prepared by spin coating or electrochemical deposition with regard to CO_2 conversion, photoelectrocatalysis was performed for 2 h, at −0.35 V in 0.1 mol L^{-1} Na_2SO_4 and under pH 6, monitoring the methanol, ethanol, ethanol, acetone, formic acid, and acetic acid formation during each process. The potential of −0.35 V was chosen based on the photoactivity of the semiconductor and aiming at maintaining the oxidation number of the copper in the complex.

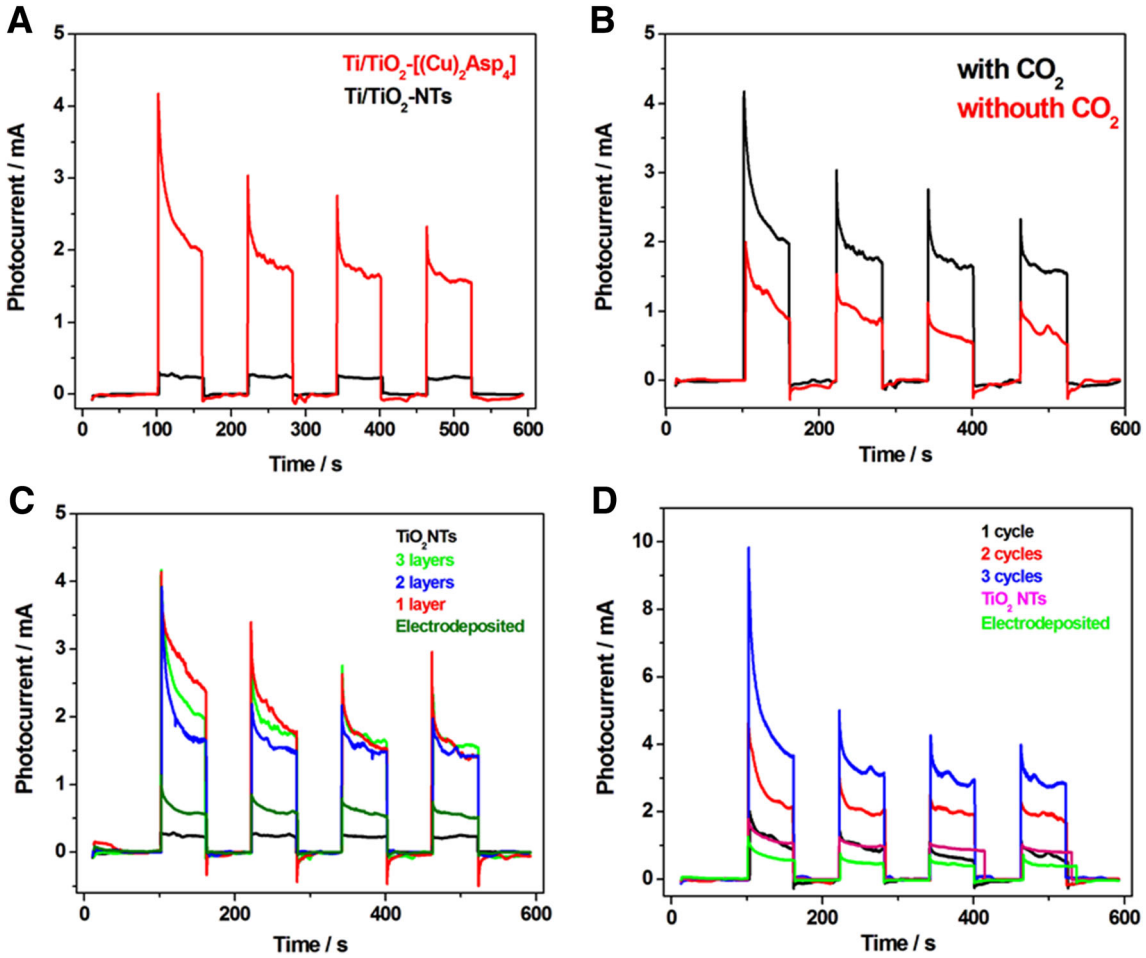

Fig. 6 Photocurrents with CO_2 (**a**); photocurrents of Ti/TiO_2-[$Cu_2(asp)_4$] with and without CO_2 (**b**); photocurrent of Ti/TiO_2 NTs and Ti/TiO_2-[$Cu_2(asp)_4$] by spin coating deposition and Ti/TiO_2-[$Cu_2(asp)_4$] by electrodeposition with CO_2 (**c**) and without CO_2 (**d**)

Figure 7a also compares the performance on the bare Ti/TiO_2 nanotube electrode. It is noteworthy that methanol was the main product formed in all the cases studied. The products, namely, ethanol, acetone, formic acid, and acetic acid, were formed in less significant quantity. The results obtained are in agreement with some works published in the literature

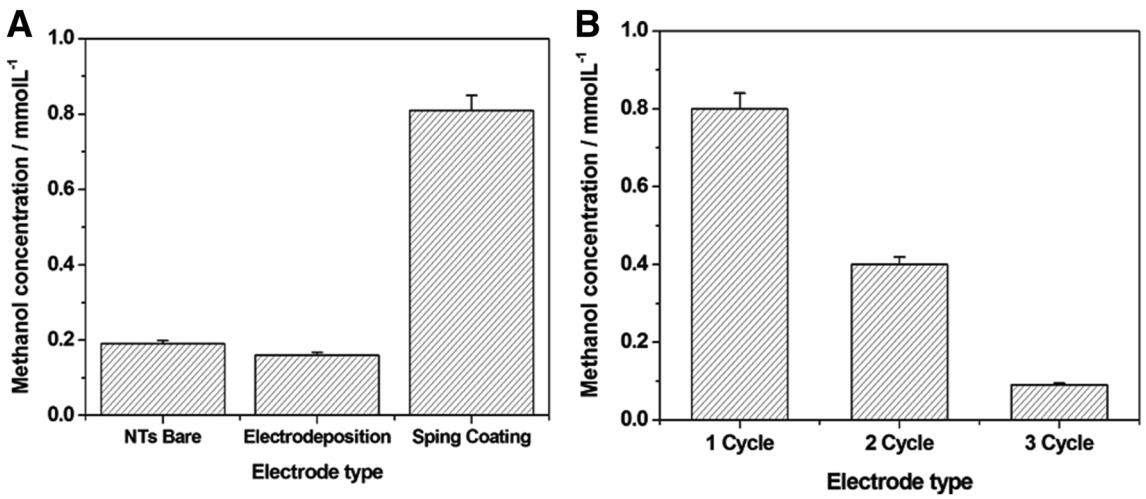

Fig. 7 Methanol formation following 120 min of photoelectrocatalytic reduction of CO_2 on bare Ti/TiO_2 NTs, Ti/TiO_2-[$Cu_2(asp)_4$] electrodeposited, and Ti/TiO_2-[$Cu_2(asp)_4$] spin coating 1 cycle (**a**) and effect of number of deposition of [$Cu_2(asp)_4$] by spin coating on methanol formation during 2 h of photoelectrocatalytic reduction of CO_2 in 0.1 mol L^{-1} sodium sulfate (**b**)

[34–36], which reported the selective methanol formation by means of CO_2 reduction using the photoelectrocatalysis technique.

In these experiments, a better result accomplished for methanol formation (0.80 mmol L^{-1}) was obtained with Ti/TiO_2-[$Cu_2(asp)_4$] prepared via spin coating. The quantity of methanol generated applying Ti/TiO_2 nanotubes and Ti/TiO_2-[$Cu_2(asp)_4$] prepared by electrochemical deposition was quite similar. This behavior induces the assumption that at the end of the [$Cu_2(asp)_4$] electrodeposition on the Ti/TiO_2 nanotube surface, no photoactivity is observed.

Figure 7b compares the CO_2 conversion as a function of the number of [$Cu_2(asp)_4$] deposition on the Ti/TiO_2 electrode using the spin coating method. The products formed in the photoelectrocatalytic CO_2 reduction also presented methanol as the major product in all of the cases, though the performance is inversely affected by the number of the complex layers on the electrode surface. This behavior can be related to the Ti/TiO_2 nanotube photoactivation. The electrons and hole pairs are generated by the light incidence on the Ti/TiO_2 nanotube surface [37]. It is worth pointing out that when the Ti/TiO_2 nanotube surface is covered by thick layers of [$Cu_2(asp)_4$], the coating can inhibit complete or partial photon absorption; as such, the electron and hole pair generation tends to be hampered. Consequently, the occurrence of a smaller electron-hole pair generation gives rise to a relatively lesser reduction of CO_2. Thus, the better option for the Ti/TiO_2-[$Cu_2(asp)_4$] electrode was found to be the spin coating deposition using one coat only.

Effect of Electrolyte Nature

One of the intrinsic challenges when it comes to CO_2 reduction lies in finding not only the better material for the purpose but also the better condition suitable for yielding the products [21]. Thus, the potential applied in the semiconductor (Fig. 8a) and a comparison between the supporting electrolytes composed of sodium sulfate and sodium bicarbonate (Fig. 8b) apart from the choice of the Ti/TiO_2-[$Cu_2(asp)_4$] electrode prepared by spin coating were all analyzed. According to Brito et al. [5], the better supporting electrolyte concentration for methanol formation is 0.1 mol L^{-1}; hence, this concentration was applied in conducting these studies.

The CO_2 reduction was carried out on Ti/TiO_2-[$Cu_2(asp)_4$] electrodes prepared by spin coating (one deposit) for 2 h at −0.35 V in 0.1 mol L^{-1} Na_2SO_4 under pH 6 along with the sodium bicarbonate solution (pH 8), where no pH correction was necessary. The results indicate that CO_2 reduction by photoelectrocatalysis presented a higher methanol formation (0.80 mmol L^{-1}) in sodium sulfate medium compared to sodium bicarbonate. Sodium sulfate was also used as supporting electrolyte for photoelectrocatalytic CO_2 reduction by Ghadimkhani et al. [35, 38]. According to the authors, using a hybrid CuO/Cu_2O electrode and sodium sulfate medium without pH adjustment, CO_2 reduction exhibited selectivity towards methanol formation. Singh and collaborators [39] affirm that a proton-limited current density presents a high value close to a neutral pH, which means a pH range of 6 to 7, and this current goes below pH 8. Thus, a pH difference in the supporting electrolytes, in effect, should not influence the results obtained. Nonetheless, many researchers in the area have stated that pH is a key factor to consider when it comes to CO_2 reduction [7, 8, 39, 40]. Spinner et al. [40] concluded that pH is the most sensitive factor and a low pH will improve the kinetics and tend to engender higher yields of reaction. According to the authors, considering a variation of pH from 7 to 6, the formation Gibbs energy tends to decrease to a negative value while the methanol concentration is found to increase by five orders of magnitude. Thus, sulfate solution was chosen in further photoelectrolysis experiments.

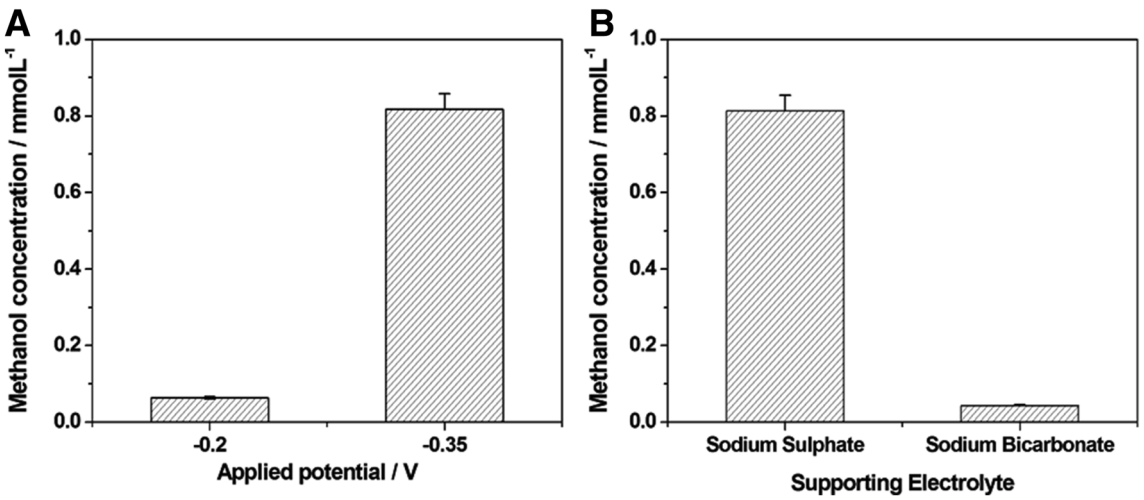

Fig. 8 Effect of applied potential (**a**) and supporting electrolyte (**b**) on the methanol formation following 120 min of photoelectrocatalysis conducted on Ti/TiO_2-[$Cu_2(asp)_4$] by spin coating

Comparison of Electrocatalysis, Photocatalysis, and Photoelectrocatalysis on the Performance of CO_2 Reduction

The influence of bias potential over the system was studied using the same photoelectrocatalytic reactor under three distinct conditions: (a) photocatalytic treatment using UV light without a bias potential, (b) electrocatalytic treatment by biasing the electrode with −0.35 V (saturated calomel electrode, SCE) in dark conditions, and (c) photoelectrocatalytic treatment, i.e., using both UV light and −0.35 V (SCE) as bias potential. A small amount of methanol (0.03 mmol L^{-1}) was quantified using electrocatalysis for the CO_2 reduction while a neglected amount of methanol was formed using photocatalysis condition. Interestingly, the methanol formation reached 0.80 mmol L^{-1} when CO_2 was reduced in sodium sulfate on Ti/TiO_2-[Cu_2(asp)$_4$] electrodes under UV irradiation and using −0.35 V as applied potential. This value is found to be much lower when the potential of −0.20 V is applied using the photoelectrocatalytic method, as demonstrated in Fig. 9a. Taking into account that Cu(II) is reduced to Cu(I) at −0.35 V on Ti/TiO_2-[Cu_2(asp)$_4$], the results indicate that Cu(II) can be reduced to Cu(I) at an applied potential of −0.35 V besides the photochemistry process by means of the electrons photogenerated through UV irradiation.

For the purpose of understanding the interference role played by the photoelectrolysis time in CO_2 conversion, the formation of methanol, ethanol, acetaldehyde, acetone, formic acid, and acetic acid was monitored during 3 h of photoelectrolysis conducted on the Ti/TiO_2-[Cu_2(asp)$_4$] electrode in sodium sulfate, E = −0.35 V irradiated by UV/Vis irradiation. During the whole photoelectrocatalysis time, none of the products was found quantified in such an expressive concentration as methanol which appeared as the major product among the lots. The results can be found in Fig. 9. Methanol formation was almost constant during the first hour of reaction (0.37 mmol L^{-1}) but was then found to increase to a higher generation value up to 2 h of reaction. Surprisingly, following 2 h of reaction, the methanol concentration started to diminish probably as a result of subsequent oxidation generating new products which were not detectable here [5, 31]. The energetic efficiency for the electrocatalysis process was 33% while for the photoelectrochemical process the energetic efficiency [41] reached 82%. These results prove the photoelectrochemical process superiority for the CO_2 reduction, being that the complex acts as mediator enabling the indirect reduction of CO_2 to methanol and subsequent oxidation of Cu(I) to Cu(II) in the complex, concomitantly to the alcohol formation. The results are graphically represented in Fig. 10.

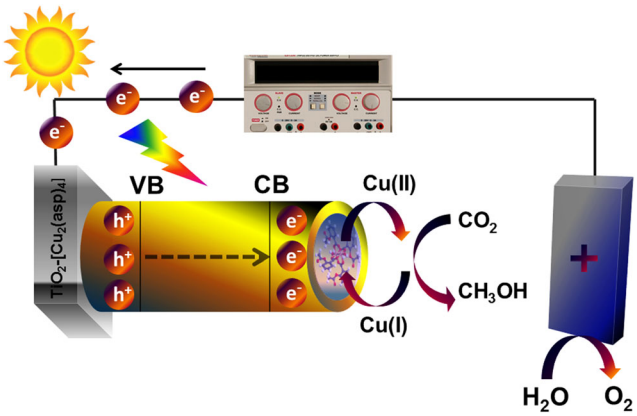

Fig. 10 Methanol formation proposal

It is a known fact in the literature that the conversion of CO_2 to highly oxidized states involves electrons, protons, and hydroxyl radicals for the formation of a great diversity of intermediate products [5, 42]. However, our finding indicates that the system adopted here leads to high selectivity to methanol.

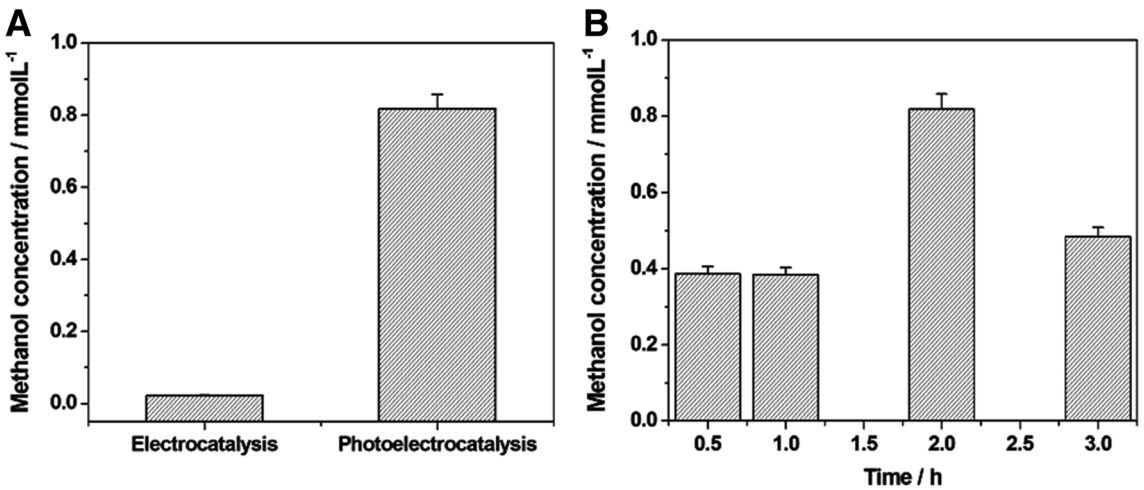

Fig. 9 Methanol formation for electrocatalysis and photoelectrocatalysis techniques (**a**) and photoelectrocatalysis during the time of CO_2 in sodium sulfate at −0.35 V and UV irradiation (**b**)

Conclusions

To sum up, we have achieved selective CO_2 photoelectrocatalytic conversion based on the decoration of Ti/TiO_2 with a copper(II) aspirinate complex. The results, we believe, may aid in enhancing the use of electron-mediating complexes when it comes to choosing photocatalysts for CO_2 reduction. The higher performance of the copper complexes associated with the photoelectrocatalytic technique may be attributed to a modification of the electronic features of Cu(II) to Cu (I) in the complex, where electrons are promoted from the valence band to the conduction band when the semiconductor is irradiated. These electrons are found to easily reach the substrate surface while being trapped by Cu(II) in the complex which is simultaneously reduced to Cu(I). The complex acts as mediator enabling the indirect reduction of CO_2 to methanol and subsequent oxidation of Cu(I) to Cu(II) in the complex. Further detailed investigations are under way aiming at proposing the reaction involved in the process. Our findings, nonetheless, provide a meaningful contribution in the search for new materials integrating the Ti/TiO_2 nanotubes, which have been well explored in the literature, with economic, simple, easily obtained, and stable copper complexes for the efficient conversion of CO_2 to an important fuel.

Acknowledgements The authors would like to express their sincerest gratitude and indebtedness to the Brazilian funding agencies FAPESP (2013/25343-8 and 2015/18109-4), CNPq (152274/2016-2 and 310421/2013-6), and CAPES for the financial support granted during the course of this research. FEG-SEM facilities were provided by LMA-IQ and X-ray diffraction measurements by GFQM-IQ. We are also grateful to Brian Newmann—the native English language content editor, for his painstaking proofreading and editing of the manuscript.

References

1. J.-R. Li, Y. Ma, M.C. McCarthy, J. Sculley, J. Yu, H.-K. Jeong, P.B. Balbuena, H.-C. Zhou, Coord. Chem. Rev. **255**, 1791 (2011)
2. N.S. Spinner, J.A. Vega, W.E. Mustain, Catal Sci Technol **2**, 19 (2012)
3. S. A. Rackley, *Carbon Capture and Storage*, 1st edn. (Butterworth-Heinemann, Elsevier, 2010), pp. 20-22
4. S.J.T. Hangx, Behaviour of the CO_2-H_2O system and preliminary mineralisation model and experiments. CATO Workpackage WP **4**, 1 (2005)
5. J.F. de Brito, A.R. Araujo, K. Rajeshwar, M.V.B. Zanoni, B. Zanoni, Chem. Eng. J. **264**, 302 (2015)
6. S. Ohya, S. Kaneco, H. Katsumata, T. Suzuki, K. Ohta, Catal. Today **148**, 329 (2009)
7. D. Gust, T.A. Moore, A.L. Moore, G. Ciamician, Faraday Discuss. **155**, 9 (2012)
8. Ş. Neaţu, J. Maciá-Agulló, H. Garcia, Int. J. Mol. Sci. **15**, 5246 (2014)
9. L. Liu, Y. Li, Aerosol Air Qual. Res. **14**, 453 (2014)
10. S. Qin, F. Xin, Y. Liu, X. Yin, W. Ma, J. Colloid Interface Sci. **356**, 257 (2011)
11. O.K. Varghese, M. Paulose, T.J. LaTempa, C.A. Grimes, Nano Lett. **9**, 731 (2009)
12. B. Srinivas, B. Shubhamangala, K. Lalitha, P. Anil Kumar Reddy, V. Durga Kumari, M. Subrahmanyam, B. R. De, Photochem. Photobiol. **87**, 995 (2011)
13. Y.-J. Yuan, Z.-T. Yu, J.-Y. Zhang, Z.-G. Zou, Dalton Trans. **41**, 9594 (2012)
14. C. Wang, X.-X. Ma, J. Li, L. Xu, F. Zhang, J. Mol. Catal. A Chem. **363**, 108 (2012)
15. S. Xie, Q. Zhang, G. Liu, Y. Wang, M. He, Y. Sun, B. Han, Chem. Commun. **52**, 35 (2016)
16. K. Rajeshwar, N.R. de Tacconi, G. Ghadimkhani, W. Chanmanee, C. Janáky, Chem Phys Chem **14**, 2005 (2013)
17. Y. Liu, L. Hua, S. Li, Desalination **258**, 48 (2010)
18. C. Finn, S. Schnittger, L.J. Yellowlees, Chem. Commun. **48**, 1392 (2012)
19. A.J. Morris, G.J. Meyer, E. Fujita, Acc. Chem. Res. **42**, 1983 (2009)
20. D. Walther, M. Ruben, S. Rau, Coord. Chem. Rev. **182**, 67 (1999)
21. G.G. Bessegato, T.T. Guaraldo, J.F. de Brito, M.F. Brugnera, M.V.B. Zanoni, Electrocatalysis **6**, 415 (2015)
22. F.M.M. Paschoal, G. Pepping, M.V.B. Zanoni, M.A. Anderson, Environmental Science & Technology **43**, 7496 (2009)
23. A.L. Abuhijleh, Inorg. Chem. Commun. **14**, 759 (2011)
24. T. Fujimori, S. Yamada, H. Yasui, H. Sakurai, Y. In, T. Ishida, Journal of Biological Inorganic Chemistry : JBIC : A Publication of the Society of Biological Inorganic Chemistry **10**, 831 (2005)
25. F.A. Sayão, J.B.S. Flor, R.C.G. Frem, S. Stulp, J.C. Cardoso, M.V.B. Zanoni, Electrocatalysis **486**, 6 (2016)
26. S. Sato, T. Arai, T. Morikawa, K. Uemura, T.M. Suzuki, H. Tanaka, T. Kajino, J. Am. Chem. Soc. **133**, 15240 (2011)
27. J.C. Cardoso, T.M. Lizier, M.V.B. Zanoni, Appl. Catal. B Environ. **99**, 96 (2010)
28. J.C. Cardoso, M.V. Boldrin Zanoni, Sep. Sci. Technol. **45**, 1628 (2010)
29. G.G. Bessegato, J.C. Cardoso, B.F. da Silva, M.V.B. Zanoni, Appl. Catal. B Environ. **180**, 161 (2016)
30. G.G. Bessegato, J.C. Cardoso, B.F. da Silva, M.V.B. Zanoni, J. Photochem. Photobiol. A Chem. **276**, 96 (2014)
31. T.T. Guaraldo, J.F. de Brito, D. Wood, M.V.B. Zanoni, Electrochim. Acta **185**, 117 (2015)
32. H.S. Kushwaha, N.A. Madhar, B. Ilahi, P. Thomas, Scientific Reports **6**, 18557 (2016)
33. J.H. Clark, M.S. Dyer, R.G. Palgrave, C.P. Ireland, J.R. Darwent, J.B. Claridge, M.J. Rosseinsky, J. Am. Chem. Soc. **133**, 1016 (2011)
34. J.F. Brito, A.A. Silva, A.J. Cavalheiro, M.V.B. Zanoni, Int. J. Electrochem. Sci. **9**, 5961 (2014)
35. G. Ghadimkhani, N.R. de Tacconi, W. Chanmanee, C. Janaky, K. Rajeshwar, Chem. Commun. (Camb.) **49**, 1297 (2013)
36. H. Peng, J. Lu, C. Wu, Z. Yang, H. Chen, W. Song, P. Li, H. Yin, Appl. Surf. Sci. **353**, 1003 (2015)
37. A. Fujishima, K. Honda, Bull. Chem. Soc. Jpn. **44**, 1148 (1971)
38. K. Rajeshwar, N.R. De Tacconi, G. Ghadimkhani, W. Chanmanee, C. Janáky, Chem Phys Chem **14**, 2251 (2013)
39. M.R. Singh, E.L. Clark, A.T. Bell, Physical Chemistry Chemical Physics : PCCP **17**, 18924 (2015)
40. N.S. Spinner, J.A. Vega, W.E. Mustain, Catalysis Science & Technology **2**, 19 (2012)
41. H.R.M. Jhong, S. Ma, P.J. Kenis, Current Opinion in Chemical Engineering **2**, 191 (2013)
42. D.M. Halmann, and M. Steinberg, *Greenhouse Gas—Carbon Dioxide Mitigation: Science and Technology*, 6th edn. (Lewis Publishers, Boca Raton, 1999), p. 61